Journal of Science and Technology, Vol. 64, 2023

ADAPTIVE NEURAL TRACKING CONTROL FOR SURFACE SHIP WITH COMPENSATED TRACKING ERROR-CONSTRAINS AND DELAY INPUT BASED ON COMMAND-FILTER

HOANG THI TU UYEN
Faculty of Electrical Engineering Technology, Industrial University of Ho Chi Minh City
hoangthituuyen@iuh.edu.vn
DOIs: https://doi.org/10.46242/jstiuh.v64i04.4891

Abstract. The article proposes an algorithm for trajectory tracking control problem of full actuated surface ships in the presence of state constraints, the delay of the input signal, and uncertain model parameters. During the design process, radial basis function neural networks are used to approximate the nonlinear components of uncertainty and a symmetric barrier Lyapunov function is incorporated to cope with the constraints of compensated tracking error. In particular, an auxiliary system is employed to eliminate the delay of the input signals, which often makes the control performance worse, even unstable. The adaptive controller that the article proposes is built based on the backstepping method using a command filter to avoid derivative explosion and reduce the computational burden on the controller. The article shows that tracking errors of surface ship can converge to a small neighborhood of zero, the compensated tracking error constraints of the system are not violated, the system is still stable when the input signal is delayed.
Keywords. Adaptive neural tracking control, Radial basis function neural networks, Auxiliary system, Command filtering backstepping, Barrier Lyapunov function.

Abbreviations

DoF	Degree of freedom	BLF	Barrier Lyapunov function
NN	Neural network	RBF	Radial basis function
DSC	Dynamic surface control	ACF	Adaptive command filter
MIMO	Multi-input and multi-output	AACF	Adaptive auxiliary system - command filter

1 INTRODUCTION

Marine surface ships have a great role in the fields of transportation, survey, monitoring, research, and restoration of the marine environment and many military applications [1-3]. Controlling marine surface ship to track a predefined trajectory when moving at sea will reduce labor, and accurate tracking has special significance in surveying the marine environment and the military. Therefore, controlling the surface ships to follow a desired trajectory has attracted more and more attention [4, 5]. However, to guarantee stability of surface ships in harsh ocean environment is a challenging problem for nonlinear control design and development. Firstly, ocean environment always contains complex, unstructured factors such as ocean currents, waves and winds, which create unpredictable disturbances for the control system. Second, the ship dynamics are highly nonlinear and contain unknown parameters or uncertain external disturbances [6, 7]. The presence of non-parametric uncertainty creates modeling errors and makes traditional model-based controllers unfeasible. Third, ship dynamics always contain multiple degrees of freedom (DoFs) and interact with each other, when noise in one DoF can propagate to other DoFs, causing performance degradation or even destabilization. In addition, the existence of input delay and the constraints are also a challenge in trajectory tracking of surface ships. The presence of input delay and state constraint in many practical engineering applications is indispensable and unavoidable, it appears in various forms such as saturation, delay of magnetic field, physical discontinuity, performance characteristics and others [8-10]. The existence of input delay and the violation of constraints could degrade the performance of control systems, even destabilizes the system, cause collisions which lead to tremendous economic loss and environmental pollution. Therefore, the control of this problem is very important in the control design process for surface ships.

For the first three problems, many control methods have been developed for surface ships. For example, the tracking control method is based on the backstepping approach, the sliding mode tracking control method is proposed based on the exact model [11, 12]. In recent years, adaptive neural network (NN) control schemes have been used to approximate complex nonlinear systems with high uncertainty due to their inherent approximation capabilities.[13-15]. Features of adaptive neural network control include: (i) the design and analysis based on Lyapunov stability theory; (ii) stability and performance of the closed-loop control system can be readily determined; (iii) neural network weights are tuned online, using a Lyapunov synthesis method, rather than optimization techniques. As a result, adaptive neural network control overcomes the disadvantage of the optimization-based neural network controller, which is difficult to derive analytical results for stability analysis and performance evaluation of the closed-loop system [16]. In many studies, the authors have designed the controller based on the backstepping approach [4, 17], the unknown nonlinear functions are approximated by the neural network. However, in the traditional backstepping approach there exists the problem of explosive complexity caused by the repeated differentiations of the virtual control signals. To solve the issue of explosive complexity and reduce the computational burden, dynamic surface control (DSC) has been proposed [18, 19]. Nevertheless, the DSC methods do not compensate for filter errors which would degrade the control performance. In order to meliorate control performance, command filtered-based adaptive backstepping control method was first presented in [20], the virtual control signal is approximated by the output signal of the command filter at each step of the backstepping control design, and filter errors were eliminated by using the compensating system. In the literature [21], the authors utilized a command filter to design the tracking controller of underactuated surface ship, but did not take into account the input delay.

Due to the physical characteristics of the actuator, the existence of delay is unavoidable in practical engineering, which makes the controller unable to respond in time to changes of system state. This causes the characteristics of system to deteriorate, even to fall into an unstable state. To solve the daedal issue, many researchers have carried out research on this problem [22, 23]. In the literature [24], the authors used the command filter algorithm in combination with the auxiliary system to tackle the input delay and saturation problem for nonlinear multi-input and multi-output (MIMO) state constrained systems.

Similar to the input delay, the state constraint problem is also a challenging task. In cases the route of ship is strictly limited by both sides of the trajectory, such as when the ship is moving through a narrow channel, or when exploring through the seas with many obstacles, the tracking error constrained problem should be considered to ensure the safety of navigation for the vehicle. There have been many studies to solve the constraint problem. Among the methods used to deal with the constraint problem, the barrier Lyapunov function (BLF) can ensure that the constraint is not violated by using the Lyapunov stability method to keep the BLF bound. Tee et al investigated the issue of time-varying output constraints by utilizing a time-varying BLF function [8]. Chen and Ge presented this control approach for MIMO systems [9], Jin et al employed this method to control fault toleration [25, 26]. It has also been used in practical applications, such as marine vessels [21, 27, 28], but the issue of input delay has been taken no account in these works.

In this brief, we present an adaptive trajectory tracking controller for a 3-DoF fully actuated surface ship with parametric or functional uncertainties, the existence of input delay and state constraints. The contributions of this brief are summarized as follows:

1) Based on adaptive neural networks to approximate the unknown nonlinear functions in dynamic model of the surface ship.

2) The tracking error constraints is tackled by BLF.

3) The input delay is handled through the auxiliary system and command filter. The integration of the command filter and the backend system into the control law also avoids the explosion of complexity.

4) It is proven that the system is stable, the output signals converge to a neighborhood of the reference trajectories, the compensated tracking error constraints are not violated, and the states of the closed system are bounded.

The rest of the brief is organized as follows. Section II introduces dynamics of 3-DoF fully actuated surface ship and preliminaries. Section III presents the steps of controller design and stability analysis. In Section

IV, a simulation example is given to illustrate the feasibility of the proposed control. Finally, a conclusion is provided in Section V.

2 PROBLEM FORMULATION AND PRELIMINARIES

Throughout this brief, $|\cdot|$ represents the absolute value of a scalar, and $\langle\cdot\rangle$ represents the absolute value of each component of a vector, i.e., for a vector $\boldsymbol{x} \in R^n$, $\langle \boldsymbol{x} \rangle = [|x_1|, |x_2|, \dots, |x_n|]^T$. In addition, $\|.\|$ represents the Euclidean norm of a vector. For a vector $\boldsymbol{a} \in R^n$, a_i $(i = 1, 2, \dots, n)$ means the corresponding ith component of a. For any vectors $\boldsymbol{a} \in R^n$ and $\boldsymbol{b} \in R^n$, $\boldsymbol{a} < \boldsymbol{b}$ means $a_i < b_i$, $i = 1, 2, \dots, n$, and $\langle \mathbf{a} \rangle < \boldsymbol{b}$ means $|a_i| < b_i$.

2.1 Problem Formulation

In this section, we consider MIMO dynamics of a 3-DoF surface ship with uncertainties. The surface ship in the horizontal plane is shown in Figure 1 [29]

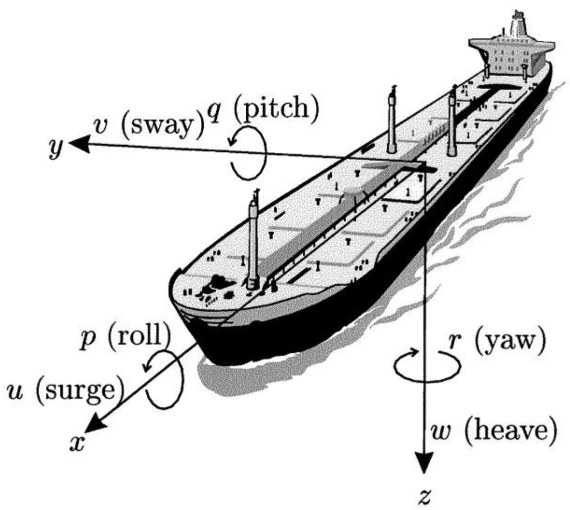

Figure 1. Motion variables for surface ship

The dynamics of a 3-DoF surface ship are described as follows [29, 30]:

$$\begin{cases} \dot{\boldsymbol{\eta}} = \boldsymbol{J}(\boldsymbol{\eta})\boldsymbol{\nu} \\ \boldsymbol{M}\dot{\boldsymbol{\nu}} + \boldsymbol{C}(\boldsymbol{\nu})\boldsymbol{\nu} + \boldsymbol{D}(\boldsymbol{\nu})\boldsymbol{\nu} + \boldsymbol{g}(\boldsymbol{\eta}) + \Delta(\boldsymbol{\eta}, \boldsymbol{\nu}) = \boldsymbol{\tau} \end{cases} \tag{1}$$

Where output $\boldsymbol{\eta} = [x, y, \psi]$ denotes position (x, y) and yaw angle around z-axis (ψ) of ship in the earth-fixed frame; $\boldsymbol{\nu} = [u, v, r]$ represents linear velocities along x-axis (u), y-axis (v) and angular velocity around z-axis (r), respectively in the body-fixed frame; $\boldsymbol{M}$ is the symmetric positive definite inertia matrix of the ship. The parameters of $\boldsymbol{M}$ are constant and are determined quite accurately [30] using semi-empirical methods or hydrodynamic computations programs; $\boldsymbol{C}(\boldsymbol{\nu})$ is the total Coriolis and centripetal acceleration matrix; $\boldsymbol{D}(\boldsymbol{\nu})$ is the damping matrix; $\boldsymbol{J}(\boldsymbol{\eta})$ is the 3DOF rotation matrix; $\boldsymbol{g}(\boldsymbol{\eta})$ is the vector of gravitational/buoyancy forces and moments; $\Delta(\boldsymbol{\eta}, \boldsymbol{\nu})$ is the vector of unknown modeling errors and environmental disturbances; $\boldsymbol{\tau} \in R^3$ is the vector of control inputs. The coefficients in the rotation matrix $\boldsymbol{J}(\boldsymbol{\eta})$ are given by:

$$\boldsymbol{J}(\boldsymbol{\eta}) = \begin{bmatrix} \cos\psi & -\sin\psi & 0 \\ \sin\psi & \cos\psi & 0 \\ 0 & 0 & 1 \end{bmatrix} \tag{2}$$

where: $\boldsymbol{J}(\boldsymbol{\eta})^T\boldsymbol{J}(\boldsymbol{\eta}) = \boldsymbol{I}$.

$$\boldsymbol{M} = \begin{bmatrix} m - X_{\dot{u}} & 0 & 0 \\ 0 & m - Y_{\dot{v}} & mx_g - Y_{\dot{r}} \\ 0 & mx_g - N_{\dot{v}} & I_z - N_{\dot{r}} \end{bmatrix} \tag{3}$$

The coefficients in the matrix $\boldsymbol{C}(\boldsymbol{\nu}), \boldsymbol{D}(\boldsymbol{\nu})$ and vectors $\boldsymbol{g}(\boldsymbol{\eta}), \Delta(\boldsymbol{\eta}, \boldsymbol{\nu})$ are given by:

$$\boldsymbol{C}(\boldsymbol{\nu}) = \begin{bmatrix} 0 & 0 & -(m - Y_{\dot{v}})v - (mx_g - Y_{\dot{r}})r \\ 0 & 0 & (m - X_{\dot{u}})u \\ (m - Y_{\dot{v}})v + (mx_g - Y_{\dot{r}})r & -(m - X_{\dot{u}})u & 0 \end{bmatrix} \tag{4}$$

$$\boldsymbol{D}(\boldsymbol{\nu}) = \boldsymbol{D} + \boldsymbol{D}_n(\boldsymbol{\nu})$$

$$\boldsymbol{D} = \begin{bmatrix} -X_u & 0 & 0 \\ 0 & -Y_v & -Y_r \\ 0 & -N_v & -N_r \end{bmatrix} \tag{5}$$

$$\boldsymbol{D}_n(\boldsymbol{\nu}) = \begin{bmatrix} -X_{|u|u}|u| & 0 & 0 \\ 0 & -Y_{|v|v}|v| - Y_{|r|v}|r| & -Y_{|v|r}|v| - Y_{|r|r}|r| \\ 0 & -N_{|v|v}|v| - N_{|r|v}|r| & -N_{|v|r}|v| - N_{|r|r}|r| \end{bmatrix}$$

$$\boldsymbol{g}(\boldsymbol{\eta}) = \begin{bmatrix} g_1(\boldsymbol{\eta}) \\ g_2(\boldsymbol{\eta}) \\ g_3(\boldsymbol{\eta}) \end{bmatrix} \ and \ \Delta(\boldsymbol{\eta}, \boldsymbol{\nu}) = \begin{bmatrix} \Delta_1(\boldsymbol{\eta}, \boldsymbol{\nu}) \\ \Delta_2(\boldsymbol{\eta}, \boldsymbol{\nu}) \\ \Delta_3(\boldsymbol{\eta}, \boldsymbol{\nu}) \end{bmatrix} \tag{6}$$

where $\boldsymbol{C}(\boldsymbol{\nu})$, $\boldsymbol{D}(\boldsymbol{\nu})$, $\boldsymbol{g}(\boldsymbol{\eta})$, $\Delta(\boldsymbol{\eta}, \boldsymbol{\nu})$ are unknown function matrices and vectors, depending on positional and velocity vector. $\{X_{(.)}, Y_{(.)}, N_{(.)}\}$ are the coefficients which represent hydrodynamic parameters according to the notation of The Society of Naval Architects and Marine Engineers [29] .

Let $\boldsymbol{x}_1 = \boldsymbol{\eta}$, $\boldsymbol{x}_2 = \boldsymbol{\nu}$ and consider the input signal of the system $\boldsymbol{\tau}(t - t_d)$ with the known time delay t_d, which satisfies $0 \le t_d \le t_{dmax}$, t_{dmax} is a known constant. Then the dynamics of the surface ship (1) can be rewritten as:

$$\begin{cases} \dot{\boldsymbol{x}}_1 = \boldsymbol{J}(\boldsymbol{x}_1)\boldsymbol{x}_2 \\ \dot{\boldsymbol{x}}_2 = \boldsymbol{M}^{-1}[\boldsymbol{\tau}(t - t_d) - \boldsymbol{C}(\boldsymbol{x}_2)\boldsymbol{x}_2 - \boldsymbol{D}(\boldsymbol{x}_2)\boldsymbol{x}_2 - \boldsymbol{g}(\boldsymbol{x}_1) - \Delta(\boldsymbol{x}_1, \boldsymbol{x}_2)] \end{cases} \tag{7}$$

The control objective of this brief is to design an adaptive NN controller for the surface ship such that: 1) the output $\boldsymbol{y}(t) = \boldsymbol{x}_1(t)$ converges to a neighborhood of the desired trajectory $\boldsymbol{y}_d(t) = \boldsymbol{x}_d(t) = [x_{d1}(t), x_{d2}(t), x_{d3}(t)]^T$ 2) all the closed-loop signals remain bounded. The following assumptions will be used to achieve our control objective.

Assumption 1: The disturbance of the environment is bounded, so there exists a positive constant vector $\boldsymbol{b} = [b_1, b_2, b_3]^T$, such that $\langle \Delta \rangle < \boldsymbol{b}$.

Assumption 2: the desired trajectory is continuous, bounded and known, so there exists a positive constant vector $\boldsymbol{k}_c = [k_{c1}, k_{c2}, k_{c3}]^T$ satisfying $\langle \boldsymbol{x}_d(t) \rangle \le \boldsymbol{k}_c$. And its first-order time derivative $\dot{\boldsymbol{x}}_d(t)$ is continuous bounded.

2.2 Preliminaries

Lemma 1.[24, 31] . For any positive constant k_{di} and variable z_i, the following inequality can be obtained, when z_i satisfies the inequality $|z_i| < k_{di}$,

$$\log \frac{k_{di}^2}{k_{di}^2 - z_i^2} \le \frac{z_i^2}{k_{di}^2 - z_i^2} \tag{8}$$

Lemma 2 [20, 24] . The command filter is proposed to avoid the explosion of complexity as follows:

$$\dot{\psi}_1 = \omega_n \psi_2 \tag{9}$$

$$\dot{\psi}_2 = -2\zeta\omega_n\psi_2 - \omega_n(\psi_1 - \alpha_1) \tag{10}$$

when the input signal α_1 satisfies $|\dot{\alpha}_1| \le \rho_1$ and $|\ddot{\alpha}_1| \le \rho_2$ for all $t \ge 0$, where $\rho_i \ge 0$, $i = 1, 2$, the initial conditions of command filter are $\psi_1(0) = \alpha_1(0)$, and $\psi_2(0) = 0$. For any positive constant β, there exists filter design parameters $\omega_n \ge 0$ and $0 \le \zeta \le 1$ such that the filter error $|\psi_1 - \alpha_1| \le \beta$ and $|\dot{\psi}_1|, |\ddot{\psi}_1|, |\dddot{\psi}_1|$ are bounded. There exists a constant ϑ satisfying $|\dot{\psi}_1| \le \vartheta$.

Lemma 3 [32] . An unknown continuous nonlinear function $f(\boldsymbol{x}) : R^m \to R$ can be approximated to arbitrary accuracy by using the radial basis function (RBF) NN on a compact set $\Omega_{\boldsymbol{x}} \subset R^m$ as follows:

$$f(\boldsymbol{x}) = W^{*T} S(\boldsymbol{x}) + \epsilon(\boldsymbol{x}), \qquad \forall \boldsymbol{x} \in \Omega_{\boldsymbol{x}} \tag{11}$$

Where $W^* = [w_1^*, \dots, w_n^*] \in R^n$ (n is node number of the NN) is the ideal constant weight vector, $\boldsymbol{x} \in R^m$ is the input vector of the NN. $\epsilon(\boldsymbol{x})$ is the approximation error satisfying $|\epsilon(x)| \le \epsilon^*(\epsilon^* > 0$ is an unknown constant). $S(\boldsymbol{x}) = [s_1(\boldsymbol{x}), \dots, s_n(\boldsymbol{x})]^T$ is the radial basis function vector where $s_i(\boldsymbol{x})$ are the Gaussian functions, which have the form:

$$s_i(\boldsymbol{x}) = exp\left[\frac{-(\boldsymbol{x} - \mu_i)^T(\boldsymbol{x} - \mu_i)}{\varsigma_i^2}\right], i = 1,2, \dots, n$$

Lemma 4 [24]. the auxiliary system defined as follows:

$$\begin{cases} \dot{\lambda}_{i,1} = \lambda_{i,2} - p_{i,1}\lambda_{i,1} \\ \dot{\lambda}_{i,j} = \lambda_{i,j+1} - p_{i,j}\lambda_{i,j} \\ \dot{\lambda}_{i,n_i} = -p_{i,n_i}\lambda_{i,n_i} + u_i\big(v_i(t - t_d)\big) - u_i(v_i(t)) \end{cases} \tag{12}$$

where $p_{i,1} > \frac{1}{2}$, $p_{i,j} > 1, p_{i,n_i} > \frac{1}{3}(i = 1,2, \dots, n; j = 2, \dots, n-1)$ are designed parameters and the initial condition of this auxiliary system is $\lambda(0) = 0$.

The auxiliary system defined in (12) has state bounded by

$$\|\lambda(t)\| \le \sqrt{\frac{2\rho}{\chi}} \tag{13}$$

where $\chi = \min\{2\left(p_{i,1} - \frac{1}{2}\right), 2\big(p_{i,j} - 1\big), 2\left(p_{i,n_i} - \frac{3}{2}\right), i = 1,2, \dots, n; \rho = \sum_{i=1}^{n} u_{Mi}^2, u_{Mi}$ is the known bound of $u_i(.)$

3 CONTROL DESIGN AND STABILITY ANALYSIS

3.1 Control Design Steps

Due to the input of the system has a delay, an auxiliary system is used to eliminate the effect of the input delay, constructed as follows:

$$\begin{cases} \dot{\boldsymbol{\lambda}}_1 = \boldsymbol{J}(\boldsymbol{x})\boldsymbol{\lambda}_2 - \boldsymbol{P}_1\boldsymbol{\lambda}_1 \\ \dot{\boldsymbol{\lambda}}_2 = -\boldsymbol{P}_2\boldsymbol{\lambda}_2 + \boldsymbol{M}^{-1}[\boldsymbol{\tau}(t - t_d) - \boldsymbol{\tau}(t)] \end{cases} \tag{14}$$

where $\boldsymbol{P}_1, \boldsymbol{P}_2$ are positive constant diagonal matrices

$$\boldsymbol{P}_1 = \begin{bmatrix} p_{1,1} & 0 & 0 \\ 0 & p_{1,2} & 0 \\ 0 & 0 & p_{1,3} \end{bmatrix}, \boldsymbol{P}_2 = \begin{bmatrix} p_{2,1} & 0 & 0 \\ 0 & p_{2,2} & 0 \\ 0 & 0 & p_{2,3} \end{bmatrix}$$

The tracking errors of the adaptive neural command-filtered control are defined:

$$\begin{cases} \boldsymbol{e}_1 = \boldsymbol{x}_1 - \boldsymbol{\lambda}_1 - \boldsymbol{x}_d \\ \boldsymbol{e}_2 = \boldsymbol{x}_2 - \boldsymbol{\lambda}_2 - \boldsymbol{x}_{2c} \end{cases} \tag{15}$$

where $\boldsymbol{x}_{2c}$ is the output vector of the command filter with the virtual controller $\boldsymbol{\alpha}_1$ as the input and $\boldsymbol{x}_d$ is the desired tracking signal vector. The command filter is described as follows:

$$\begin{cases} \dot{\boldsymbol{x}}_{2c} = \omega_n\boldsymbol{x}_{2d} \\ \dot{\boldsymbol{x}}_{2d} = -2\zeta\omega_n\boldsymbol{x}_{2d} - \omega_n(\boldsymbol{x}_{2c} - \boldsymbol{\alpha}_1) \end{cases} \tag{16}$$

where according to the *Lemma 2*: $\omega_n \ge 0$ and $0 \le \zeta \le 1$

Due to the command filter can create filtering errors which affect the dynamic characteristics of the system, so it is necessary to use the error compensation to eliminate the filtering errors. Let $\boldsymbol{\xi}_1$ is the error compensation signal vector defined as:

$$\dot{\boldsymbol{\xi}}_1 = -\boldsymbol{C}_1\boldsymbol{\xi}_1 + \boldsymbol{J}(\boldsymbol{x}_1)(\boldsymbol{x}_{2c} - \boldsymbol{\alpha}_1) = (\dot{\xi}_{1,1}, \dot{\xi}_{1,2}, \dot{\xi}_{1,3})^T \tag{17}$$

where $\boldsymbol{C}_1$ is a positive constant diagonal matrix:

$$\boldsymbol{C}_1 = \begin{bmatrix} c_{1,1} & 0 & 0 \\ 0 & c_{1,2} & 0 \\ 0 & 0 & c_{1,3} \end{bmatrix}$$

According to the Lemma 4 in [20], the outputs of system (17) are bounded $\langle \boldsymbol{\xi}_1 \rangle \leq \frac{\boldsymbol{\beta}}{2\kappa_0}$ where according *Lemma 2*, $\boldsymbol{\beta}$ is boundedness of the input $\langle (\boldsymbol{x}_{2c} - \boldsymbol{\alpha}_1) \rangle < \boldsymbol{\beta}$, $\kappa_0 = 0.5\min\{c_{1,1}, c_{1,2}, c_{1,3}\}$
Then the compensated tracking error signals are defined as:

$$\begin{cases} \boldsymbol{z}_1 = \boldsymbol{e}_1 - \boldsymbol{\xi}_1 \\ \boldsymbol{z}_2 = \boldsymbol{e}_2 \end{cases} \tag{18}$$

The controller is designed in the following sequence:
Step 1: Choose the Lyapunov function as:

$$V_1 = \sum_{i=1}^{3} \frac{1}{2} log \frac{k_{d1,i}^2}{k_{d1,i}^2 - z_{1,i}^2} \tag{19}$$

where $k_{d1,i}$ denotes the predefined constraint of compensated tracking error $z_{1,i}$ and $k_{d1,i}$ is the design positive constant.
The derivative of V_1 is:

$$\dot{V}_1 = \sum_{i=1}^{3} \frac{z_{1,i}.\dot{z}_{1,i}}{k_{d1,i}^2 - z_{1,i}^2} \tag{20}$$

According to (18):

$$\boldsymbol{z}_1 = \boldsymbol{e}_1 - \boldsymbol{\xi}_1$$

The time derivative of $\boldsymbol{z}_1$ can be obtained:

$$\dot{\boldsymbol{z}}_1 = \dot{\boldsymbol{e}}_1 - \dot{\boldsymbol{\xi}}_1 = \dot{\boldsymbol{x}}_1 - \dot{\boldsymbol{\lambda}}_1 - \dot{\boldsymbol{x}}_d - \dot{\boldsymbol{\xi}}_1$$

$$\dot{\boldsymbol{z}}_1 = \boldsymbol{J}(\boldsymbol{x}_1)\boldsymbol{x}_2 - \boldsymbol{J}(\boldsymbol{x}_1)\boldsymbol{\lambda}_2 + \boldsymbol{P}_1\boldsymbol{\lambda}_1 - \dot{\boldsymbol{x}}_d - \dot{\boldsymbol{\xi}}_1$$

$$\dot{\boldsymbol{z}}_1 = \boldsymbol{J}(\boldsymbol{x}_1)(\boldsymbol{x}_2 - \boldsymbol{\lambda}_2) + \boldsymbol{P}_1\boldsymbol{\lambda}_1 - \dot{\boldsymbol{x}}_d - \dot{\boldsymbol{\xi}}_1$$

$$\dot{\boldsymbol{z}}_1 = \boldsymbol{J}(\boldsymbol{x}_1)(\boldsymbol{e}_2 + \boldsymbol{x}_{2c}) + \boldsymbol{P}_1\boldsymbol{\lambda}_1 - \dot{\boldsymbol{x}}_d - \dot{\boldsymbol{\xi}}_1$$

$$\dot{\boldsymbol{z}}_1 = \boldsymbol{J}(\boldsymbol{x}_1)(\boldsymbol{z}_2 + \boldsymbol{x}_{2c}) + \boldsymbol{P}_1\boldsymbol{\lambda}_1 - \dot{\boldsymbol{x}}_d - \dot{\boldsymbol{\xi}}_1$$

$$\dot{\boldsymbol{z}}_1 = \boldsymbol{J}(\boldsymbol{x}_1)(\boldsymbol{z}_2 + \boldsymbol{x}_{2c} - \boldsymbol{\alpha}_1 + \boldsymbol{\alpha}_1) + \boldsymbol{P}_1\boldsymbol{\lambda}_1 - \dot{\boldsymbol{x}}_d - \dot{\boldsymbol{\xi}}_1 \tag{21}$$

The virtual control vector $\boldsymbol{\alpha}_1$ is designed as:

$$\boldsymbol{\alpha}_1 = \boldsymbol{J}^{\boldsymbol{T}}(\boldsymbol{x}_1)(\dot{\boldsymbol{x}}_d - \boldsymbol{C}_1\boldsymbol{e}_1 - \boldsymbol{P}_1\boldsymbol{\lambda}_1) = (\alpha_{1,1}, \alpha_{1,2}, \alpha_{1,3})^T \tag{22}$$

Substituting (17),(22) to (21), we have:

$$\begin{aligned} \dot{\boldsymbol{z}}_1 = \boldsymbol{J}(\boldsymbol{x}_1).\boldsymbol{z}_2 + \boldsymbol{J}(\boldsymbol{x}_1)(\boldsymbol{x}_{2c} - \boldsymbol{\alpha}_1) + \boldsymbol{J}(\boldsymbol{x}_1)\boldsymbol{J}^{\boldsymbol{T}}(\boldsymbol{x}_1)(\dot{\boldsymbol{x}}_d - \boldsymbol{C}_1\boldsymbol{e}_1 - \boldsymbol{P}_1\boldsymbol{\lambda}_1) + \boldsymbol{P}_1\boldsymbol{\lambda}_1 \\ - \dot{\boldsymbol{x}}_d + \boldsymbol{C}_1\boldsymbol{\xi}_1 - \boldsymbol{J}(\boldsymbol{x}_1)(\boldsymbol{x}_{2c} - \boldsymbol{\alpha}_1) \end{aligned} \tag{23}$$

$$\dot{\boldsymbol{z}}_1 = \boldsymbol{J}(\boldsymbol{x}_1).\boldsymbol{z}_2 - \boldsymbol{C}_1\boldsymbol{z}_1 \tag{24}$$

From (24), we have:

$$\dot{V}_1 = \sum_{i=1}^{3} -\frac{c_{1,i}.z_{1,i}^2}{k_{d1,i}^2 - z_{1,i}^2} + \sum_{i=1}^{3} \frac{z_{1,i}.\boldsymbol{J}_{\boldsymbol{i}}(\boldsymbol{x}_1).\boldsymbol{z}_2}{k_{d1,i}^2 - z_{1,i}^2} \tag{25}$$

Step 2:
According to (18)

$$\boldsymbol{z}_2 = \boldsymbol{e}_2 = \boldsymbol{x}_2 - \boldsymbol{\lambda}_2 - \boldsymbol{x}_{2c} \tag{26}$$

The time derivative of $\boldsymbol{z}_2$:

$$\dot{\boldsymbol{z}}_2 = \dot{\boldsymbol{x}}_2 - \dot{\boldsymbol{\lambda}}_2 - \dot{\boldsymbol{x}}_{2c} \tag{27}$$

$$\begin{aligned} \dot{\boldsymbol{z}}_2 = \boldsymbol{M}^{-\boldsymbol{1}}[\boldsymbol{\tau}(t - t_d) - \boldsymbol{C}(\boldsymbol{x}_2)\boldsymbol{x}_2 - \boldsymbol{D}(\boldsymbol{x}_2)\boldsymbol{x}_2 - \boldsymbol{g}(\boldsymbol{x}_1) - \Delta(\boldsymbol{x}_1, \boldsymbol{x}_2)] \\ + \boldsymbol{P}_2\boldsymbol{\lambda}_2 - \boldsymbol{M}^{-\boldsymbol{1}}[\boldsymbol{\tau}(t - t_d) - \boldsymbol{\tau}(t)] - \dot{\boldsymbol{x}}_{2c} \end{aligned} \tag{28}$$

$$\dot{\boldsymbol{z}}_2 = \boldsymbol{M}^{-1}[\boldsymbol{\tau}(t) - \boldsymbol{C}(\boldsymbol{x}_2)\boldsymbol{x}_2 - \boldsymbol{D}(\boldsymbol{x}_2)\boldsymbol{x}_2 - \boldsymbol{g}(\boldsymbol{x}_1) - \Delta(\boldsymbol{x}_1, \boldsymbol{x}_2) + \boldsymbol{M}\boldsymbol{P}_2\boldsymbol{\lambda}_2 - \boldsymbol{M}\dot{\boldsymbol{x}}_{2c}] \tag{29}$$

The control law is chosen as follows:

$$\boldsymbol{\tau}(t) = \boldsymbol{C}(\boldsymbol{x}_2)\boldsymbol{x}_2 + \boldsymbol{D}(\boldsymbol{x}_2)\boldsymbol{x}_2 + \boldsymbol{g}(\boldsymbol{x}_1) + \Delta(\boldsymbol{x}_1, \boldsymbol{x}_2) + \boldsymbol{M}\dot{\boldsymbol{x}}_{2c} - \boldsymbol{C}_2\boldsymbol{e}_2 - \boldsymbol{M}\boldsymbol{P}_2\boldsymbol{\lambda}_2 - \sum_{i=1}^{3} \frac{z_{1,i}.\boldsymbol{J}_i^T(\boldsymbol{x}_2)}{k_{d1,i}^2 - z_{1,i}^2} \tag{30}$$

where $\boldsymbol{C}_2$ is a positive constant diagonal matrix:

$$\boldsymbol{C}_2 = \begin{bmatrix} c_{2,1} & 0 & 0 \\ 0 & c_{2,2} & 0 \\ 0 & 0 & c_{2,3} \end{bmatrix}$$

The control law (30) can only be implemented when the model parameter matrices $\boldsymbol{C}(\boldsymbol{x}_2)$, $\boldsymbol{D}(\boldsymbol{x}_2)$, $\boldsymbol{g}(\boldsymbol{x}_1)$, $\Delta(\boldsymbol{x}_1, \boldsymbol{x}_2)$ are well known. However, as seen in [29, 30] the accurate determination of the matrices and vectors $\boldsymbol{C}(\boldsymbol{x}_2)$, $\boldsymbol{D}(\boldsymbol{x}_2)$, $\boldsymbol{g}(\boldsymbol{x}_1)$, $\Delta(\boldsymbol{x}_1, \boldsymbol{x}_2)$ and the measured error of the sensors are very difficult. The article collects the uncertain components into an uncertain function vector, which is approximated by the RBF neural network.

The uncertain function vector is expressed as:

$$\boldsymbol{F}(\boldsymbol{l}) = -\big(\boldsymbol{C}(\boldsymbol{x}_2)\boldsymbol{x}_2 + \boldsymbol{D}(\boldsymbol{x}_2)\boldsymbol{x}_2 + \boldsymbol{g}(\boldsymbol{x}_1) + \Delta(\boldsymbol{x}_1, \boldsymbol{x}_2)\big) = [f_1(\boldsymbol{l}), f_2(\boldsymbol{l}), f_3(\boldsymbol{l})]^T \in R^3 \tag{31}$$

By employing the RBF NN to approximate the unknown function $f_i(\boldsymbol{l}) \in R, i = 1,2,3,$ $f_i(\boldsymbol{l})$ can be expressed as:

$$f_i(\boldsymbol{l}) = \boldsymbol{W}_i^{*T}\boldsymbol{Q}(\boldsymbol{l}) + \epsilon_i(\boldsymbol{l}) \quad i = 1,2,3 \tag{32}$$

where $\boldsymbol{W}_i^* \in R^n$ denotes the ideal constant weights, $|\epsilon_i(\boldsymbol{l})| \le \epsilon_i^*$ are NN approximation errors with constants $\epsilon_i^* > 0$. Due to $\boldsymbol{W}_i^*$ is unknown so we let $\widehat{W}_i$ be the estimate of W_i^*, $\widehat{\boldsymbol{F}}(\boldsymbol{l})$ be the estimate of $\boldsymbol{F}(\boldsymbol{l})$.

$$\widehat{\boldsymbol{F}}(\boldsymbol{l}) = \widehat{\boldsymbol{W}}^T\boldsymbol{Q}(\boldsymbol{l}) = [\hat{f}_1(\boldsymbol{Q}(\boldsymbol{l}), \widehat{\boldsymbol{W}}_1), \hat{f}_2(\boldsymbol{Q}(\boldsymbol{l}), \widehat{\boldsymbol{W}}_2), \hat{f}_3(\boldsymbol{Q}(\boldsymbol{l}), \widehat{\boldsymbol{W}}_3)]^T \tag{33}$$

The (29) can be rewritten as:

$$\dot{\boldsymbol{z}}_2 = \boldsymbol{M}^{-1}[\boldsymbol{\tau} + \boldsymbol{F}(\boldsymbol{l}) + \boldsymbol{M}\boldsymbol{P}_2\boldsymbol{\lambda}_2 - \boldsymbol{M}\dot{\boldsymbol{x}}_{2c}] \tag{34}$$

$$\dot{\boldsymbol{z}}_2 = \boldsymbol{M}^{-1}[\boldsymbol{\tau} + \boldsymbol{W}^{*T}\boldsymbol{Q}(\boldsymbol{l}) + \boldsymbol{\epsilon}(\boldsymbol{l}) + \boldsymbol{M}\boldsymbol{P}_2\boldsymbol{\lambda}_2 - \boldsymbol{M}\dot{\boldsymbol{x}}_{2c}] \tag{35}$$

where $\boldsymbol{W}^{*T}\boldsymbol{Q}(\boldsymbol{l}) = [\boldsymbol{W}_1^{*T}\boldsymbol{Q}(\boldsymbol{l}), \boldsymbol{W}_2^{*T}\boldsymbol{Q}(\boldsymbol{l}), \boldsymbol{W}_3^{*T}\boldsymbol{Q}(\boldsymbol{l})]^T$, $\boldsymbol{\epsilon}(\boldsymbol{l}) = [\epsilon_1(\boldsymbol{l}), \epsilon_2(\boldsymbol{l}), \epsilon_3(\boldsymbol{l})]^T$, $\widehat{\boldsymbol{W}}^T\boldsymbol{Q}(\boldsymbol{l}) = [\widehat{\boldsymbol{W}}_1^T\boldsymbol{Q}(\boldsymbol{l}), \widehat{\boldsymbol{W}}_2^T\boldsymbol{Q}(\boldsymbol{l}), \widehat{\boldsymbol{W}}_3^T\boldsymbol{Q}(\boldsymbol{l})]^T$, the input vector of NN $\boldsymbol{l} = [\boldsymbol{x}_1{}^T, \boldsymbol{x}_2{}^T]^T \in R^6$.

The feedback control is expressed as:

$$\boldsymbol{\tau}(t) = -\widehat{\boldsymbol{F}}(\boldsymbol{l}) - \boldsymbol{C}_2\boldsymbol{e}_2 + \boldsymbol{M}\dot{\boldsymbol{x}}_{2c} - \boldsymbol{M}\boldsymbol{P}_2\boldsymbol{\lambda}_2 - \sum_{i=1}^{3} \frac{z_{1,i}.\boldsymbol{J}_i^T(\boldsymbol{x}_2)}{k_{d1,i}^2 - z_{1,i}^2} \tag{36}$$

$$\boldsymbol{\tau}(t) = -\widehat{\boldsymbol{W}}^T\boldsymbol{Q}(\boldsymbol{l}) - \boldsymbol{C}_2\boldsymbol{e}_2 + \boldsymbol{M}\dot{\boldsymbol{x}}_{2c} - \boldsymbol{M}\boldsymbol{P}_2\boldsymbol{\lambda}_2 - \sum_{i=1}^{3} \frac{z_{1,i}.\boldsymbol{J}_i^T(\boldsymbol{x}_2)}{k_{d1,i}^2 - z_{1,i}^2} \tag{37}$$

Consider the following adaptive law:

$$\dot{\widehat{\boldsymbol{W}}}_i = \dot{\widetilde{\boldsymbol{W}}}_i = \boldsymbol{\Gamma}_i[\boldsymbol{Q}(\boldsymbol{l})z_{2i} - \sigma\widehat{\boldsymbol{W}}_i], i = 1,2,3 \tag{38}$$

where $\widetilde{\boldsymbol{W}}_i = \widehat{\boldsymbol{W}}_i - \boldsymbol{W}_i^*$, $\boldsymbol{\Gamma}_i = \boldsymbol{\Gamma}_i^T$ are adaptation gain matrices $\boldsymbol{\Gamma}_i \in R^{n\times n}$ và σ is a positive design parameter.

Substituting (37) to (35), we have:

$$\dot{\boldsymbol{z}}_2 = \boldsymbol{M}^{-1}[-\widehat{\boldsymbol{W}}^T\boldsymbol{Q}(\boldsymbol{l}) - \boldsymbol{C}_2\boldsymbol{e}_2 - \sum_{i=1}^{3} \frac{z_{1,i}.\boldsymbol{J}_i^T(\boldsymbol{x}_2)}{k_{d1,i}^2 - z_{1,i}^2} + \boldsymbol{W}^{*T}\boldsymbol{Q}(\boldsymbol{l}) + \boldsymbol{\epsilon}(\boldsymbol{l})] \tag{39}$$

$$\dot{\boldsymbol{z}}_2 = \boldsymbol{M}^{-1}[-\boldsymbol{C}_2\boldsymbol{e}_2 - \sum_{i=1}^{3} \frac{z_{1,i}.\boldsymbol{J}_i^T(\boldsymbol{x}_2)}{k_{d1,i}^2 - z_{1,i}^2} - \widetilde{\boldsymbol{W}}^T\boldsymbol{Q}(\boldsymbol{l}) + \boldsymbol{\epsilon}(\boldsymbol{l})] \tag{40}$$

Consider the Lyapunov function as:

$$V = V_1 + \frac{1}{2}\boldsymbol{z}_2^T \boldsymbol{M} \boldsymbol{z}_2 + \frac{1}{2}\sum_{i=1}^{3} \widetilde{\boldsymbol{W}}_i^T \boldsymbol{\Gamma}_i^{-1} \widetilde{\boldsymbol{W}}_i \tag{41}$$

The derivative of V is:

$$\dot{V} = \dot{V}_1 + \boldsymbol{z}_2^T \boldsymbol{M} \dot{\boldsymbol{z}}_2 + \sum_{i=1}^{3} \widetilde{\boldsymbol{W}}_i^T \boldsymbol{\Gamma}_i^{-1} \dot{\widetilde{\boldsymbol{W}}}_i \tag{42}$$

$$\begin{aligned}\dot{V} = \sum_{i=1}^{3} -\frac{c_{1,i}.z_{1,i}^2}{k_{d1,i}^2 - z_{1,i}^2} + \sum_{i=1}^{3} \frac{z_{1,i}.\boldsymbol{J_i}(\boldsymbol{x}_1).\boldsymbol{z}_2}{k_{d1,i}^2 - z_{1,i}^2} + \bar{z}_2^T \boldsymbol{M}\boldsymbol{M}^{-1}[-\boldsymbol{C}_2 \boldsymbol{e}_2 - \sum_{i=1}^{3} \frac{z_{1,i}.\boldsymbol{J}_i^T(\boldsymbol{x}_2)}{k_{d1,i}^2 - z_{1,i}^2} \\ - \widetilde{W}^T \boldsymbol{Q}(\boldsymbol{l}) + \boldsymbol{\epsilon}(\boldsymbol{l})] + \sum_{i=1}^{3} \widetilde{\boldsymbol{W}}_i^T \boldsymbol{\Gamma}_i^{-1} \dot{\widetilde{\boldsymbol{W}}}_i\end{aligned} \tag{43}$$

$$\begin{aligned}\dot{V} = \sum_{i=1}^{3} -\frac{c_{1,i}.z_{1,i}^2}{k_{d1,i}^2 - z_{1,i}^2} + \sum_{i=1}^{3} \frac{z_{1,i}.\boldsymbol{J_i}(\boldsymbol{x}_1).\boldsymbol{z}_2}{k_{d1,i}^2 - z_{1,i}^2} - \boldsymbol{z}_2^T \boldsymbol{C}_2 \boldsymbol{e}_2 - \sum_{i=1}^{3} \frac{z_{1,i}.\boldsymbol{J_i}(\boldsymbol{x}_1).\boldsymbol{z}_2}{k_{d1,i}^2 - z_{1,i}^2} \\ - \sum_{i=1}^{3} \widetilde{\boldsymbol{W}}_i^T \boldsymbol{Q}(\boldsymbol{l}) z_{2,i} + \bar{z}_2^T \boldsymbol{\epsilon}(\boldsymbol{l}) + \sum_{i=1}^{3} \widetilde{\boldsymbol{W}}_i^T \boldsymbol{\Gamma}_i^{-1} \boldsymbol{\Gamma}_i [\boldsymbol{Q}(\boldsymbol{l}) z_{2i} - \sigma \widehat{\boldsymbol{W}}_i]\end{aligned} \tag{44}$$

$$\dot{V} = \sum_{i=1}^{3} -\frac{c_{1,i}.z_{1,i}^2}{k_{d1,i}^2 - z_{1,i}^2} - \boldsymbol{z}_2^T \boldsymbol{C}_2 \boldsymbol{e}_2 + \boldsymbol{z}_2^T \boldsymbol{\epsilon}(\boldsymbol{l}) - \sum_{i=1}^{3} \widetilde{\boldsymbol{W}}_i^T \sigma \widehat{\boldsymbol{W}}_i \tag{45}$$

By using Young's inequality:

$$\boldsymbol{z}_2^T \boldsymbol{\epsilon} \le \boldsymbol{z}_2^T \boldsymbol{z}_2 + \frac{1}{4}\boldsymbol{\epsilon}^T \boldsymbol{\epsilon} \le \boldsymbol{z}_2^T \boldsymbol{z}_2 + \frac{1}{4}\boldsymbol{\epsilon}^{*T} \boldsymbol{\epsilon}^* \tag{46}$$

Therewith, we have:

$$2\widetilde{\boldsymbol{W}}_i^T \widehat{\boldsymbol{W}}_i \ge \left\|\widetilde{\boldsymbol{W}}_i\right\|^2 - \|\boldsymbol{W}_i^*\|^2 \tag{47}$$

Then, we have the following inequality:

$$\dot{V} \le \sum_{i=1}^{3} -\frac{c_{1,i}.z_{1,i}^2}{k_{d1,i}^2 - z_{1,i}^2} - \boldsymbol{z}_2^T (\boldsymbol{C}_2 - I) \boldsymbol{z}_2 - \frac{\sigma}{2}\sum_{i=1}^{3} \left(\left\|\widetilde{\boldsymbol{W}}_i\right\|^2 - \|\boldsymbol{W}_i^*\|^2\right) + \frac{1}{4}\boldsymbol{\epsilon}^{*T} \boldsymbol{\epsilon}^* \tag{48}$$

Choose:

$$\boldsymbol{C}_1 = \boldsymbol{K}_0$$
$$\boldsymbol{C}_2 = \boldsymbol{K}_0/2 + I$$

where $\boldsymbol{K}_0$ is a positive definite matrix, $\boldsymbol{K}_0 = [k_{01} \ \ 0 \ \ 0; 0 \ \ k_{02} \ \ 0; 0 \ \ 0 \ \ k_{03}]$

$$\dot{V} \le -\sum_{i=1}^{3} \frac{k_{0i}.z_{1,i}^2}{k_{d1,i}^2 - z_{1,i}^2} - \frac{1}{2}\boldsymbol{z}_2^T \boldsymbol{K}_0 \boldsymbol{z}_2 - \frac{\sigma}{2}\sum_{i=1}^{3} \left\|\widetilde{\boldsymbol{W}}_i\right\|^2 + \left(\frac{1}{4}\boldsymbol{\epsilon}^{*T} \boldsymbol{\epsilon}^* + \frac{\sigma}{2}\sum_{i=1}^{3} \|\boldsymbol{W}_i^*\|^2\right) \tag{49}$$

According to Lemma 1, we have:

$$-\frac{k_{0i}.z_{1,i}^2}{k_{d1,i}^2 - z_{1,i}^2} \le -k_{0i} \log \frac{k_{d1,i}^2}{k_{d1,i}^2 - z_{1,i}^2}$$

The (49) can be rewritten as:

$$\begin{aligned}\dot{V} \le -\sum_{i=1}^{3} k_{0i} \log \frac{k_{d1,i}^2}{k_{d1,i}^2 - z_{1,i}^2} - \frac{1}{2}\boldsymbol{z}_2^T \boldsymbol{K}_0 \boldsymbol{z}_2 - \frac{\sigma}{2\lambda_{max}(\Gamma_i^{-1})}\sum_{i=1}^{3} \widetilde{\boldsymbol{W}}_i^T \Gamma_i^{-1} \widetilde{\boldsymbol{W}}_i \\ + \left(\frac{1}{4}\boldsymbol{\epsilon}^{*T} \boldsymbol{\epsilon}^* + \frac{\sigma}{2}\sum_{i=1}^{3} \|\boldsymbol{W}_i^*\|^2\right)\end{aligned} \tag{50}$$

Choose σ so that:

$$k_0 = \lambda_{min}(\boldsymbol{K}_0)$$
$$\frac{\sigma}{\lambda_{max}(\Gamma_i^{-1})} = k_0$$

$$\Rightarrow \quad \dot{V} \le -k_0 V + b \tag{51}$$

where $b = \frac{1}{4}\boldsymbol{\epsilon}^{*T}\boldsymbol{\epsilon}^{*} + \frac{\sigma}{2}\sum_{i=1}^{3}\|\boldsymbol{W}_i^{*}\|^2$

According to (51), we can get:

$$V(t) \le V(0)e^{-at} + \frac{b}{k_0}(1 - e^{-at}) \tag{52}$$

So, the following inequality holds:

$$\frac{1}{2}\log\frac{k_{d1,i}^2}{k_{d1,i}^2 - z_{1,i}^2} \le V(t) \le V(0)e^{-at} + \frac{b}{k_0}(1 - e^{-at}) \tag{53}$$

$$\frac{k_{d1,i}^2}{k_{d1,i}^2 - z_{1,i}^2} \le e^{2\left(V(0) - \frac{b}{k_0}\right)e^{-at} + 2\frac{b}{k_0}} \tag{54}$$

$$k_{d1,i}^2 \le (e^{2\left(V(0) - \frac{b}{k_0}\right)e^{-at} + 2\frac{b}{k_0}})(k_{d1,i}^2 - z_{1,i}^2) \tag{55}$$

$$\left|z_{1,i}(t)\right| \le k_{d1,i}\sqrt{1 - e^{-2\left(V(0) - \frac{b}{k_0}\right)e^{-at} - 2\frac{b}{k_0}}} < k_{d1,i} \tag{56}$$

3.2 Stability Analysis

The main result of this brief: Consider the surface ship (7) with Assumptions 1 and 2 for initial conditions starting under the virtual controller (22), the adaptive law (38) and the actual controller (37), then the system has the following properties:

1) All the closed-loop state signals are bounded

2) The output tracking error $\boldsymbol{y}(t) - \boldsymbol{y}_d(t)$ can be adjusted around the origin with an arbitrarily small neighborhood.

Proof:

1) From the inequality (51) results in ultimately uniformly bounded stabilization of $\boldsymbol{z}_1, \boldsymbol{z}_2, \widetilde{\boldsymbol{W}}_i$ and since b is arbitrary, the boundedness of these states can be made arbitrarily small.

The expression (56) shows that the value of $\boldsymbol{z}_1$ is bounded $\langle \boldsymbol{z}_1 \rangle < \boldsymbol{k}_{d1}$, the constrained value of compensated tracking error is never violated. When increasing the value of k_0 and decreasing the value of b (by decreasing σ), the bounded of $z_{1,i}$ will be smaller, results in smaller output tracking error ($\boldsymbol{y}(t) - \boldsymbol{y}_d(t)$).

Based on (18) and the boundedness of $\boldsymbol{\xi}_1$, we can deduce that $\langle \boldsymbol{e}_1 \rangle < \boldsymbol{k}_{d1} + \langle \boldsymbol{\xi}_1 \rangle$ is bounded. Due to the physical characteristics of the actuator, $\boldsymbol{\tau}$ are saturated signals so according to Lemma 4, $\boldsymbol{\lambda}_1, \boldsymbol{\lambda}_1$ are bounded. From (15), Assumption 2 and Lemma 4, we know that $\langle \boldsymbol{x}_1 \rangle < \boldsymbol{k}_{d1} + \langle \boldsymbol{\xi}_1 \rangle + \boldsymbol{k}_c + \langle \boldsymbol{\lambda}_1 \rangle \le \boldsymbol{k}_{a1}$. According to Assumption 1 and equation (22), the virtual control signal vector includes functions of bounded signals $\boldsymbol{e}_1, \dot{\boldsymbol{x}}_d, \boldsymbol{\lambda}_1$, so $\boldsymbol{\alpha}_1$ is a bounded vector. Similarly, from equation (18) we have $\boldsymbol{e}_2 = \boldsymbol{z}_2$, so $\boldsymbol{e}_2$ is a bounded vector. Because of the command filter error satisfying $\langle(\boldsymbol{x}_{2c} - \boldsymbol{\alpha}_1)\rangle < \boldsymbol{\beta}$**,** the output signal $\boldsymbol{x}_{2c}$ of the filter is also bounded. So $\boldsymbol{x}_2 \le \langle \boldsymbol{e}_2 \rangle + \langle \boldsymbol{\lambda}_2 \rangle + \langle \boldsymbol{x}_{2c} \rangle \le \boldsymbol{k}_{a1}$, is a bounded vector. Due to $\widetilde{\boldsymbol{W}}_i$ are bounded so $\widehat{\boldsymbol{W}}_i = \widetilde{\boldsymbol{W}}_i + \boldsymbol{W}_i^{*}$ are bounded. From (37), it can be concluded that the feedback control laws are also bounded since $\boldsymbol{Q}(\boldsymbol{l})$ are bounded for all values of the NN input $\boldsymbol{l}$. Therefore, all the signals in the closed-loop system remain bounded.

2) According to Eq (15), (18) the output tracking error can be represented as $\boldsymbol{y} - \boldsymbol{y}_d = \boldsymbol{x}_1 - \boldsymbol{x}_d(t) = \boldsymbol{e}_1 + \boldsymbol{\lambda}_1 = \boldsymbol{z}_1 + \boldsymbol{\xi}_1 + \boldsymbol{\lambda}_1 \le \langle \boldsymbol{z}_1 \rangle + \langle \boldsymbol{\xi}_1 \rangle + \langle \boldsymbol{\lambda}_1 \rangle$. By choosing the appropriate design parameters as $k_0, \sigma, \boldsymbol{P}_1, \boldsymbol{P}_2$, the output tracking errors can be adjusted around the origin with arbitrarily small neighborhoods.

4 SIMULATION

To demonstrate the effectiveness of the proposed control design, we perform a numerical simulation on the system (7). The model used for simulation is the Cybership II, which is a 1:70 scale supply vessel replica built in a marine control laboratory in the Norwegian University of Science and Technology [30].

The known inertia matrix parameters of ship [30] are given by:

$M = [25.800\ 0\ 0; 0\ 25.6612\ 1.0948; 0\ 1.0948\ 2.7600]$

The initial states: $\eta(0) = [[0.02; 1; 0.02]]^T$, $\nu(0) = [0.2,0,0]^T$, $\eta_d(0) = [0,1,0]^T$. The reference trajectory: $\eta_d = [\sin(t), \cos(t), \sin(t)]^T$.
We construct the Gaussian RBF NN $\widehat{\boldsymbol{W}}_i^T \boldsymbol{Q}(\boldsymbol{l})$ using 6400 nodes, with the centers evenly spaced on [-3.8, 3.8]x[-3.8, 3.8]x[-3, 3] and the width $\varsigma_i = 0.8$, $i = 1, 2, 3$. The designed parameters are $\boldsymbol{K}_0$ = [24 0 0;0 24 0;0 0 16]; $\boldsymbol{\Gamma}_1 = 10, \boldsymbol{\Gamma}_2 = 10, \boldsymbol{\Gamma}_3 = 3$. The initial weights of the neural network are set as: $\widehat{\boldsymbol{W}}_1 = \widehat{\boldsymbol{W}}_2 = \widehat{\boldsymbol{W}}_3 = 0$
The other parameters are designed as follows: ω_n = [35 0 0;0 35 0;0 0 80]; ζ = 1; P_1 = [1.4 0 0;0 1.4 0;0 0 3]; P_2 = [8 0 0;0 10 0;0 0 8]; k_{d1}=0.05; k_{d2}=0.05; k_{d3}=0.05; delay time $t_d = 50 \times sample\ cycle$; $sample\ cycle = 0.002(s)$
Two cases are simulated to evaluate the impact of the auxiliary system when the system has an input delay. The first, when the adaptive neural system is equipped only command filter without an auxiliary system (ACF), the input signal has no delay, the system is stable, without violating the compensated tracking error constraints. In this case, when the input signal is delayed, the system becomes unstable. The second, when the system is equipped both command filter and auxiliary system (AACF), the system remains stable when there is an input delay.
Figure 3 shows that when the AACF system has an input delay, the system is still stable and can track the reference trajectory with precision in similar to the ACF system in Figure 2. However in Figure 5, we can see that the output tracking error of the AACF system fluctuates more than the output tracking error of the ACF system in Figure 4, but after a very small initial period of time, the output tracking error is only within ±0.05[m][rad].
Figure 7 shows that the control input signals of the AACF system in an initial small period of time (0.1s) fluctuate larger than the control signals of the ACF system, and then, these control signals are the same as to the control signals of the ACF system.
Figure 9 shows that compensated tracking errors of the AACF system fluctuate more than compensated tracking errors of the ACF system in Figure 8 but do not violate the constraint.

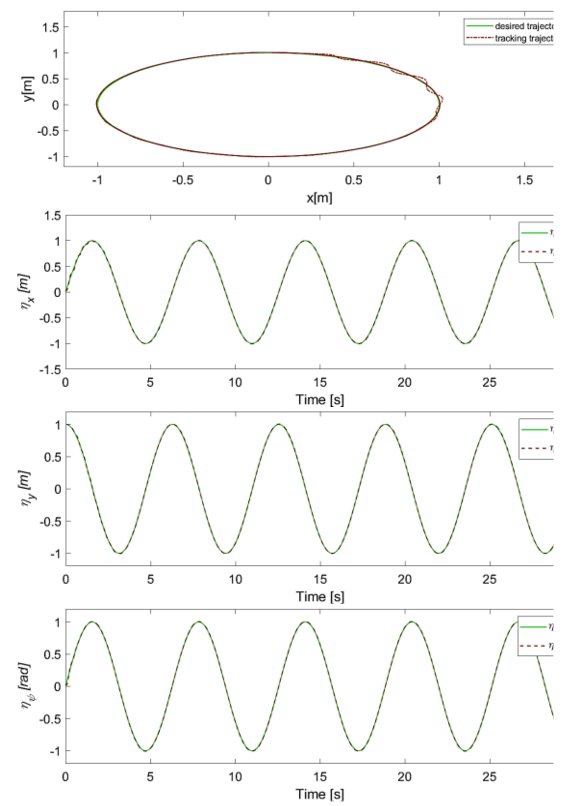

Figure 2. tracking trajectory of the ACF system

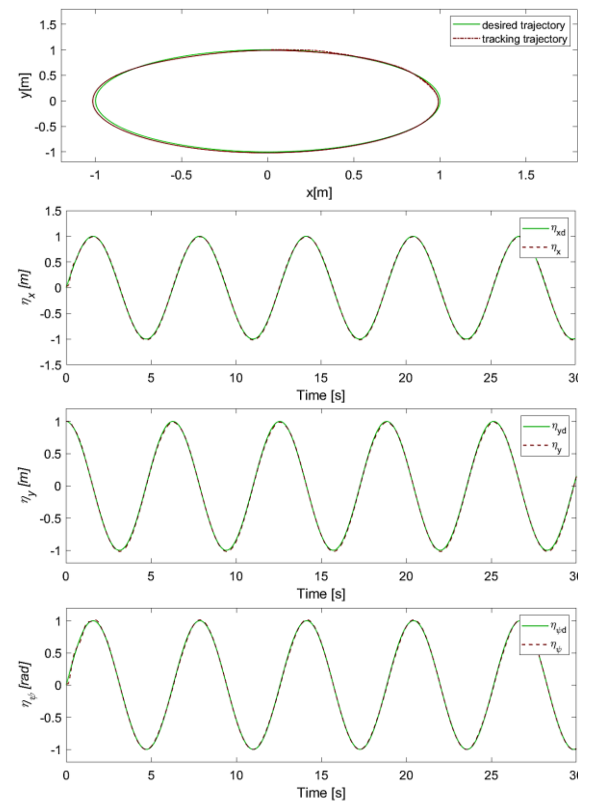

Figure 3. tracking trajectory of the AACF system

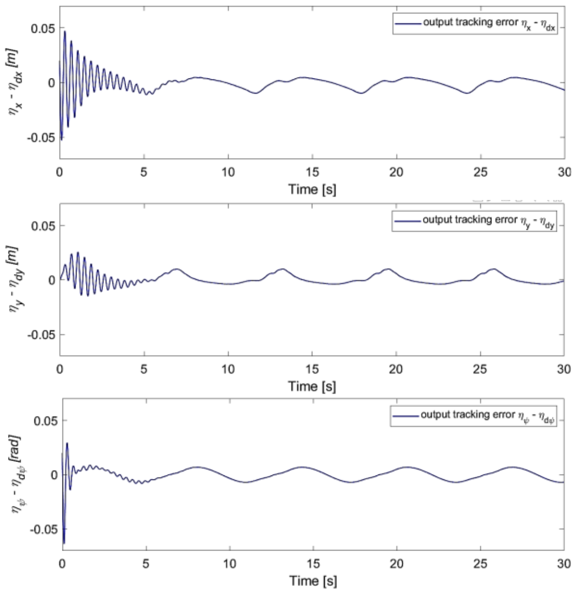

Figure 4. output tracking errors of the ACF system

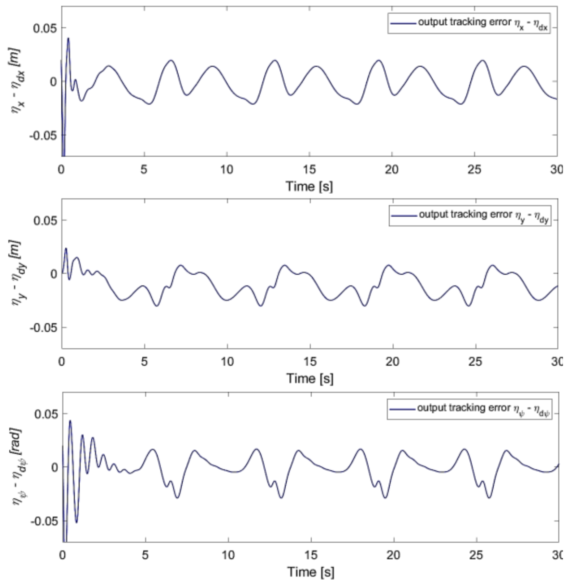

Figure 5. output tracking errors of the AACF system

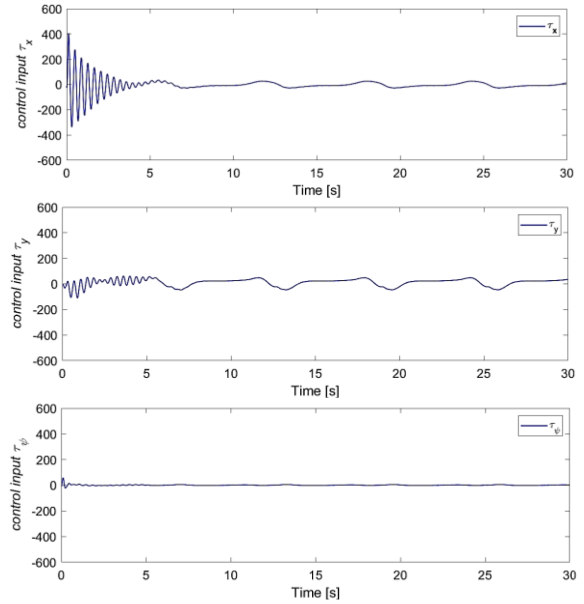

Figure 7. control inputs of the ACF system

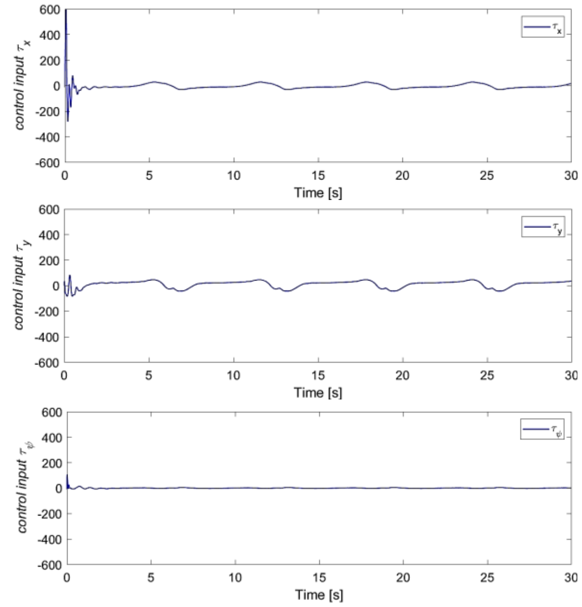

Figure 6. control inputs of the AACF system

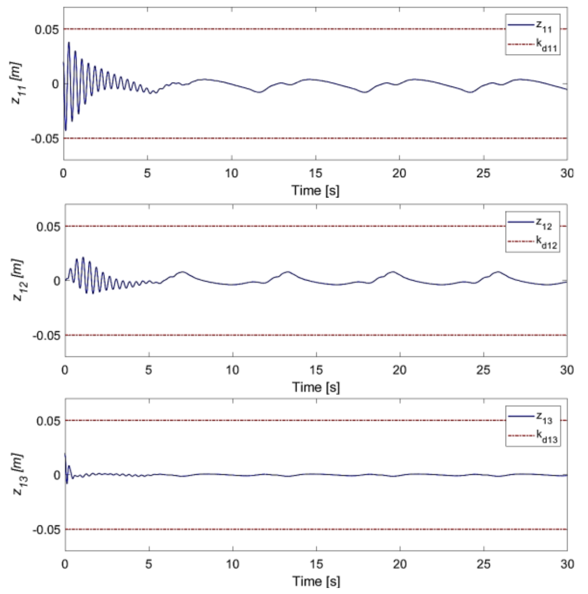

Figure 9. constrained constant and compensated tracking errors of the ACF system

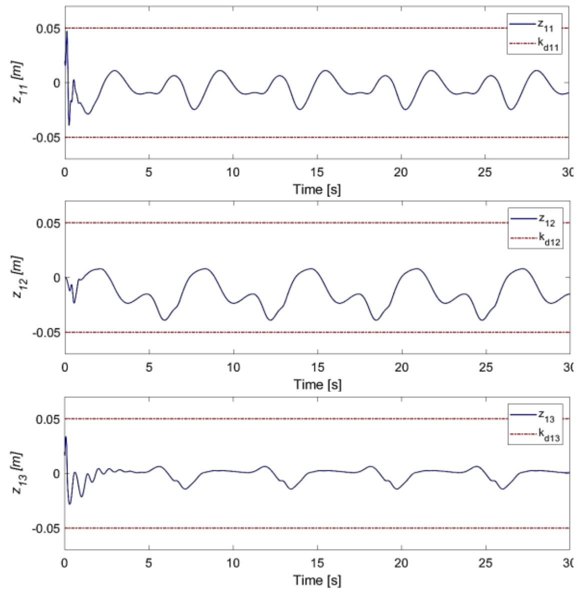

Figure 8. constrained constant and compensated tracking errors of the AACF system

5 CONCLUSION

In this paper, an adaptive neural controller based on a command filter is used for the trajectory tracking problem of surface ship in the presence of state constraints and delay of the input signal. The constraints of compensated tracking errors are dealt with by suitable barrier Lyapunov functions. The influence of input delay on the control system is rejected by the auxiliary system. The command filter-based backstepping control method is utilized to reduce the computational burden, avoiding complexity explosion. With the proposed approach, we proved that the system is stable, the output signals track the desired trajectories with the output tracking errors converge to the neighborhood of zero, and the constraints of the compensated tracking error are not violated. Simulations verified the tracking performance of the proposed method.

REFERENCES

[1] J. Kristensen and K. Vestgard, "*Hugin-an untethered underwater vehicle for seabed surveying*," in IEEE Oceanic Engineering Society. OCEANS'98. Conference Proceedings (Cat. No. 98CH36259), 1998, vol. 1, pp. 118-123: IEEE.

[2] K. Asakawa, J. Kojima, Y. Kato, S. Matsumoto, and N. Kato, "*Autonomous underwater vehicle AQUA EXPLORER 2 for inspection of underwater cables*," in Proceedings of the 2000 International Symposium on Underwater Technology (Cat. No. 00EX418), 2000, pp. 242-247: IEEE.

[3] W. He, S. S. Ge, B. V. E. How, and Y. S. Choo, Dynamics and control of mechanical systems in offshore engineering. Springer, 2014.

[4] S.-L. Dai, C. Wang, and F. J. I. T. o. I. I. Luo, "*Identification and learning control of ocean surface ship using neural networks*," IEEE Transactions on Industrial Informatics, vol. 8, no. 4, pp. 801-810, 2012.

[5] Y. Yang, J. Du, H. Liu, C. Guo, and A. J. I. T. o. C. S. T. Abraham, "*A trajectory tracking robust controller of surface vessels with disturbance uncertainties*," IEEE Transactions on Control Systems Technology, vol. 22, no. 4, pp. 1511-1518, 2013.

[6] S. S. Ge, W. He, B. V. E. How, and Y. S. J. I. T. o. C. S. T. Choo, "*Boundary control of a coupled nonlinear flexible marine riser*," IEEE Transactions on Control Systems Technology, vol. 18, no. 5, pp. 1080-1091, 2009.

[7] W. He, S. Zhang, and S. S. J. I. T. o. I. E. Ge, "*Boundary control of a flexible riser with the application to marine installation*," IEEE Transactions on Industrial Electronics, vol. 60, no. 12, pp. 5802-5810, 2013.

[8] K. P. Tee, B. Ren, and S. S. J. A. Ge, "*Control of nonlinear systems with time-varying output constraints*," Automatica, vol. 47, no. 11, pp. 2511-2516, 2011.

[9] M. Chen, S. S. Ge, and B. J. A. Ren, "*Adaptive tracking control of uncertain MIMO nonlinear systems with input constraints*," Automatica, vol. 47, no. 3, pp. 452-465, 2011.
[10] S. Ling, H. Wang, and P. X. J. A. Liu, "*Adaptive tracking control of high-order nonlinear systems under asymmetric output constraint*," Automatica, vol. 122, p. 109281, 2020.
[11] J. M. Godhavn, T. I. Fossen, S. P. J. I. J. o. A. C. Berge, and S. Processing, "*Non- linear and adaptive backstepping designs for tracking control of ships*," International Journal of Adaptive Control Signal Processing, vol. 12, no. 8, pp. 649-670, 1998.
[12] H. Ashrafiuon, K. R. Muske, L. C. McNinch, and R. A. J. I. t. o. i. e. Soltan, "*Sliding-mode tracking control of surface vessels*," IEEE Transactions on Industrial Electronics, vol. 55, no. 11, pp. 4004-4012, 2008.
[13] S. S. Ge and C. J. I. T. o. N. N. Wang, "*Direct adaptive NN control of a class of nonlinear systems*," IEEE Transactions on Neural Networks, vol. 13, no. 1, pp. 214-221, 2002.
[14] T. Orlowska-Kowalska and M. J. I. t. o. I. I. Kaminski, "*FPGA implementation of the multilayer neural network for the speed estimation of the two-mass drive system*," IEEE Transactions on Industrial Informatics, vol. 7, no. 3, pp. 436-445, 2011.
[15] T. Orlowska-Kowalska and K. J. I. T. o. I. E. Szabat, "*Neural-network application for mechanical variables estimation of a two-mass drive system*," IEEE Transactions on Industrial Electronics, vol. 54, no. 3, pp. 1352-1364, 2007.
[16] S. S. Ge, C. C. Hang, T. H. Lee, and T. Zhang, Stable adaptive neural network control. Springer Science & Business Media, 2013.
[17] K. P. Tee and S. S. J. I. T. o. C. S. T. Ge, "*Control of fully actuated ocean surface vessels using a class of feedforward approximators*," IEEE Transactions on Control Systems Technology, vol. 14, no. 4, pp. 750-756, 2006.
[18] D. Swaroop, J. K. Hedrick, P. P. Yip, and J. C. J. I. t. o. a. c. Gerdes, "*Dynamic surface control for a class of nonlinear systems*," IEEE Transactions on Automatic Control, vol. 45, no. 10, pp. 1893-1899, 2000.
[19] J. C. Gerdes and J. K. J. J. D. S. Hedrick, Meas., Control, "*"loop-at-a-time" design of dynamic surface controllers for nonlinear systems*," J. Dyn. Sys., Meas., Control, vol. 124, no. 1, pp. 104-110, 2002.
[20] W. Dong, J. A. Farrell, M. M. Polycarpou, V. Djapic, and M. J. I. T. o. C. S. T. Sharma, "*Command filtered adaptive backstepping*," IEEE Transactions on Control Systems Technology, vol. 20, no. 3, pp. 566-580, 2011.
[21] M. Fu, T. Wang, and C. J. I. A. Wang, "*Adaptive neural-based finite-time trajectory tracking control for underactuated marine surface vessels with position error constraint*," IEEE Access, vol. 7, pp. 16309-16322, 2019.
[22] M. Krstic, "*Input delay compensation for forward complete and strict-feedforward nonlinear systems*," IEEE Transactions on Automatic Control, vol. 55, no. 2, pp. 287-303, 2009.
[23] B. Niu, L. J. I. T. o. N. N. Li, and L. Systems, "*Adaptive backstepping-based neural tracking control for MIMO nonlinear switched systems subject to input delays*," IEEE Transactions on Neural Networks, vol. 29, no. 6, pp. 2638-2644, 2017.
[24] Y. Zhou, X. Wang, and R. J. N. N. Xu, "*Command-filter-based adaptive neural tracking control for a class of nonlinear MIMO state-constrained systems with input delay and saturation*," Neural Networks vol. 147, pp. 152-162, 2022.
[25] X. J. I. J. o. R. Jin and N. Control, "*Adaptive fault tolerant control for a class of input and state constrained MIMO nonlinear systems*," International Journal of Robust Nonlinear Control, vol. 26, no. 2, pp. 286-302, 2016.
[26] X. J. A. Jin, "*Fault tolerant finite-time leader–follower formation control for autonomous surface vessels with LOS range and angle constraints*," Automatica, vol. 68, pp. 228-236, 2016.
[27] Z. Zhao, W. He, and S. S. J. I. T. o. C. S. T. Ge, "*Adaptive neural network control of a fully actuated marine surface vessel with multiple output constraints*," IEEE Transactions on Control Systems Technology, vol. 22, no. 4, pp. 1536-1543, 2013.
[28] W. He, Z. Yin, and C. J. I. t. o. c. Sun, "*Adaptive neural network control of a marine vessel with constraints using the asymmetric barrier Lyapunov function*," IEEE transactions on cybernetics, vol. 47, no. 7, pp. 1641-1651, 2016.
[29] T. I. Fossen, "*Marine control systems–guidance. navigation, and control of ships, rigs and underwater vehicles*," Marine Cybernetics, Trondheim, Norway, Org. Number NO 985 195 005 MVA, 2002.
[30] R. Skjetne, T. I. Fossen, and P. V. J. A. Kokotović, "*Adaptive maneuvering, with experiments, for a model ship in a marine control laboratory*," Automatica, vol. 41, no. 2, pp. 289-298, 2005.
[31] J. A. Farrell, M. Polycarpou, M. Sharma, and W. J. I. T. o. A. C. Dong, "*Command filtered backstepping*," IEEE Transactions on Automatic Control, vol. 54, no. 6, pp. 1391-1395, 2009.
[32] J. Park and I. W. J. N. c. Sandberg, "*Universal approximation using radial-basis-function networks*," Neural computation, vol. 3, no. 2, pp. 246-257, 1991.

ĐIỀU KHIỂN BÁM NƠ-RON THÍCH NGHI CHO TÀU BỀ MẶT CÓ RÀNG BUỘC TRẠNG THÁI VÀ ĐẦU VÀO CÓ TRỄ DỰA TRÊN BỘ LỌC LỆNH

HOÀNG THỊ TÚ UYÊN*
Khoa Công nghệ Điện, Trường Đại học Công nghiệp Thành phố Hồ Chí Minh
hoangthituuyen@iuh.edu.vn

Tóm tắt. Bài báo đề xuất thuật toán cho bài toán bám quỹ đạo của tàu bề mặt đủ cơ cấu chấp hành có yêu cầu ràng buộc trạng thái, sự trễ của tín hiệu đầu vào và thông số mô hình bất định. Trong quá trình thiết kế, mạng nơ-ron hướng tâm được sử dụng để xấp xỉ những thành phần bất định phi tuyến, hàm barrier Lyapunov đối xứng được sử dụng để khắc phục ràng buộc về sai số bám đã được bù. Đặc biệt bài báo sử dụng hệ thống phụ để loại bỏ ảnh hưởng trễ của tín hiệu đầu vào khi mà tín hiệu này có thể làm đặc tính bám của hệ thống xấu đi, thậm trí làm hệ thống mất ổn định. Bộ điều khiển thích nghi mà bài báo đề xuất được xây dựng dựa trên phương pháp backstepping có sự dụng bộ lọc lệnh nhằm tránh sự bùng nổ đạo hàm và giảm bớt gánh nặng tính toán cho bộ điều khiển. Ngoài ra, sai số do bộ lọc lệnh gây ra sẽ được bù để cải thiện đặc tính bám. Bài báo sẽ chứng minh, bộ điều khiển đề xuất có sai số bám hội tụ tới lân cận điểm không, những ràng buộc về sai số bám đã được bù của hệ thống không bị vi phạm, hệ thống vẫn ổn định khi tín hiệu đầu vào có trễ.

Từ khóa. Điều khiển bám nơ-ron thích nghi, Mạng nơ-ron hàm hướng tâm, Hệ thống phụ, Kỹ thuật backstepping có sử dụng bộ lọc lệnh, Hàm Lyapunov Barrier.

Received on: 11/11/2022

Accepted on: 29/03/2023